ments of gas-phase species used as tracers (*39*) indicate that the layers had been transported from the tropics. Such layered profiles are typical of the lower mid-latitude stratosphere in fall, winter, and spring (our summertime data are too few to allow general interpretation). Other analyses of tracer measurements have shown that quasi-horizontal transport from the near-tropopause region of the tropics occurs rapidly in fall, winter, and spring to the mid-latitudes between the tropopause and altitudes of at least 19 km (*38*, *40*). Together, these observations indicate that particles produced in the upper tropical troposphere are frequently transported to the lower mid-latitude stratosphere, where they may significantly affect particle number and surface area mixing ratios.

REFERENCES AND NOTES

1. C. E. Junge, C. W. Chagnon, J. E. Manson, *J. Meteorol.* **18**, 81 (1961).
2. R. P. Turco, R. C. Whitten, O. B. Toon, *Rev. Geophys. Space Phys.* **20**, 233 (1982).
3. V. A. Mohnen, *J. Aerosol Sci.* **47**, 1933 (1990).
4. D. W. Fahey *et al.*, *Nature* **363**, 509 (1993).
5. J. C. Wilson *et al.*, *Science* **261**, 1140 (1993).
6. M. Mozurkewich and J. G. Calvert, *J. Geophys. Res.* **93**, 15889 (1988); D. R. Hanson and A. R. Ravishankara, *ibid.* **96**, 17307 (1991).
7. M. A. Tolbert, *Science* **264**, 527 (1994).
8. D. W. Fahey *et al.*, *Nature* **344**, 321 (1990); B. W. Gandrud *et al.*, *Geophys. Res. Lett.* **17**, 457 (1990).
9. P. J. Crutzen, *Geophys. Res. Lett.* **3**, 73 (1976); M. Chin and D. D. Davis, *Global Biogeochem. Cycles* **7**, 321 (1993); *J. Geophys. Res.* **100**, 8993 (1995).
10. P. Hamill, R. P. Turco, C. S. Kiang, O. B. Toon, R. C. Whitten, *J. Aerosol Sci.* **13**, 561 (1982).
11. S. A. McKeen, S. C. Liu, C. S. Kiang, *J. Geophys. Res.* **89**, 4873 (1984).
12. H. H. Jonsson *et al.*, *ibid.*, in press.
13. A. Golombek and R. G. Prinn, *J. Atmos. Chem.* **16**, 179 (1993).
14. In the mid-latitudes, particle formation occurs occasionally near an altitude of 30 km, well above the Junge layer [J. M. Rosen and D. J. Hofmann, *J. Geophys. Res.* **88**, 3725 (1983)]. Particles also form in descending air in the polar vortices [J. C. Wilson *et al.*, *J. Geophys. Res.* **94**, 16437 (1989); D. J. Hofmann, *Geophys. Res. Lett.* **17**, 357 (1990); J. Zhao, O. B. Toon, R. P. Turco, *J. Geophys. Res.* **100**, 5215 (1995)]; the stratospheric lifetime of these particles is short as a result of their transport (*16*). Because of atmospheric transport, neither of these particle sources have significant impact on the particle NMR in the lower stratosphere.
15. D. M. Hunten, R. P. Turco, O. B. Toon, *J. Atmos. Sci.* **37**, 1342 (1980); R. P. Turco, O. B. Toon, P. Hamill, R. C. Whitten, *J. Geophys. Res.* **86**, 1113 (1981); A. Krieger and F. Arnold, *Geophys. Res. Lett.* **19**, 2301 (1992).
16. P. J. Sheridan, C. A. Brock, J. C. Wilson, *Geophys. Res. Lett.* **21**, 2587 (1994).
17. K. H. Rosenlof, *J. Geophys. Res.* **100**, 5173 (1995).
18. J. M. Rosen, D. J. Hofmann, K. H. Käselau, *J. Appl. Meteorol.* **17**, 1737 (1978).
19. J. Goodman *et al.*, *Geophys. Res. Lett.* **9**, 609 (1982); V. R. Oberbeck *et al.*, *ibid.* **8**, 18 (1981).
20. We used data collected as part of the Stratosphere-Troposphere Exchange Project of 1987 (STEP 87), the Airborne Antarctic Ozone Experiment of 1987 (AAOE), the Stratospheric Photochemistry, Aerosol, and Dynamics Experiment of 1993 (SPADE), the Airborne Southern Hemisphere Ozone Experiment of 1994 (ASHOE), and the Measurements for Assessing the Effects of Stratospheric Aircraft missions of 1994 (MAESA). Data from STEP 87 were taken from flights to, around, and from Darwin, Australia, whereas only flights to and from Panama were used from the AAOE data set. The SPADE flights were based from Moffett Field, California, and the ASHOE and MAESA flights were made from Moffett Field to Christchurch, New Zealand, with transit flights to Hawaii and Fiji. Measurements within the polar vortices have been excluded from this data set.
21. J. C. Wilson, J. H. Hyun, E. D. Blackshear, *J. Geophys. Res.* **88**, 6781 (1983).
22. D. M. Murphy *et al.*, *ibid.* **98**, 8751 (1993).
23. P. J. Sheridan, unpublished data. The elemental analysis technique (field-emission scanning transmission electron microscopy) was limited to elements with atomic masses greater than that of C. For the small particles analyzed, sensitivity was insufficient to detect elements lighter than Na or heavier elements present in only trace amounts.
24. J. M. Hoell *et al.*, *J. Geophys. Res.* **98**, 23291 (1993).
25. P. Hamill, C. S. Kiang, R. D. Cadle, *J. Atmos. Sci.* **34**, 150 (1977).
26. A. Laaksonen, V. Talanquer, D. W. Oxtobe, *Ann. Rev. Phys. Chem.*, in press.
27. K. R. Chan, S. G. Scott, T. P. Bui, S. Bowen, J. Day, *J. Geophys. Res.* **94**, 11573 (1989); K. K. Kelley *et al.*, *ibid.*, p. 317.
28. O. B. Toon, personal communication.
29. B. Gary, *J. Geophys. Res.* **94**, 11223 (1989).
30. P. B. Russell, L. Pfister, H. B. Selkirk, *ibid.* **98**, 8563 (1993).
31. R. G. Knollenberg, K. K. Kelly, J. C. Wilson, *ibid.*, p. 8639.
32. P. W. Mote *et al.*, *Geophys. Res. Lett.* **22**, 1093 (1995).
33. K. H. Rosenlof, personal communication.
34. D. Cadle and C. S. Kiang, *Rev. Geophys. Space Phys.* **15**, 195 (1977).
35. F. Gelbard and J. H. Seinfeld, *J. Colloid Interface Sci.* **78**, 485 (1980).
36. Mid-latitude aerosol characteristics were taken from a profile measured on 29 December 1988 (*5*).
37. N. H. Farlow, D. M. Hayes, H. Y Lem, *J. Geophys. Res.* **82**, 4921 (1977); N. H. Farlow, K. G. Snetsinger, D. M. Hayes, H. Y. Lem, B. M. Tooper, *ibid.* **83**, 6207 (1978); J. P. Friend, *Tellus* **28**, 467 (1965); E. K. Bigg, *J. Atmos. Sci.* **32**, 910 (1975); D. Hayes, K. Snetsinger, G. Ferry, V. Oberbeck, N. Farlow, *Geophys. Res. Lett.* **7**, 974 (1980).
38. K. A. Boering *et al.*, *Geophys. Res. Lett.* **21**, 2567 (1994).
39. S. Gaines, Ed., "Stratospheric Photochemistry, Aerosols and Dynamics Expedition," *NASA/HSRP-001* [data on CD-ROM] (NASA Ames Research Center 245-3, Moffet Field, CA, 1994).
40. E. J. Hintsa *et al.*, *Geophys. Res. Lett.* **21**, 2559 (1994).
41. C. M. Volk *et al.*, personal communication.

42. The contributions of K. H. Rosenlof, C. M. Volk, P. J. Sheridan, K. A. Boering, F. Gelbard, and O. B. Toon are gratefully acknowledged. Data were collected under several grants from the National Aeronautics and Space Administration (NASA); analysis was supported by NASA grant NCC 2-782.

10 July 1995; accepted 17 October 1995

Transcription Against an Applied Force

Hong Yin, Michelle D. Wang, Karel Svoboda, Robert Landick, Steven M. Block, Jeff Gelles*

The force produced by a single molecule of *Escherichia coli* RNA polymerase during transcription was measured optically. Polymerase immobilized on a surface was used to transcribe a DNA template attached to a polystyrene bead 0.5 micrometer in diameter. The bead position was measured by interferometry while a force opposing translocation of the polymerase along the DNA was applied with an optical trap. At saturating nucleoside triphosphate concentrations, polymerase molecules stalled reversibly at a mean applied force estimated to be 14 piconewtons. This force is substantially larger than those measured for the cytoskeletal motors kinesin and myosin and exceeds mechanical loads that are estimated to oppose transcriptional elongation in vivo. The data are consistent with efficient conversion of the free energy liberated by RNA synthesis into mechanical work.

RNA polymerases play a critical role in gene expression by synthesizing RNA transcripts containing genetic information copied from DNA templates. The nascent RNA chain is elongated in a chemical reaction during which appropriate ribonucleoside triphosphates (NTPs) are condensed with the RNA 3′ end and pyrophosphate anions (PP_i) are released. RNA polymerases move along DNA while copying it, advancing on average a distance of 1 base pair (bp) (~0.34 nm along the DNA helix axis) for each nucleotide added to the transcript [(*1*) but see also (*2*, *3*)]. In vivo, this movement performs mechanical work against hydrodynamic drag and other external forces (*4*, *5*) and therefore requires a source of free energy. The energy is provided by the condensation reaction itself, which is energetically favorable at physiological NTP and PP_i concentrations (*1*). Thus, RNA polymerases may be viewed as molecular motors that catalyze a biosynthetic reaction while using a portion of the excess free energy from the reaction to perform mechanical work. Although translocation of RNA polymerase molecules along DNA has been detected by microscopy (*6*–*8*), little is known about the ability of these enzymes to move against opposing forces or about their energy conversion effi-

H. Yin and J. Gelles, Department of Biochemistry, Biophysics Program, and Center for Complex Systems, Brandeis University, Waltham, MA 02254, USA.
M. D. Wang and S. M. Block, Department of Molecular Biology and Princeton Materials Institute, Princeton University, Princeton, NJ 08544, USA.
K. Svoboda, Biological Computation Department, AT&T Bell Laboratories, Murray Hill, NJ 07974, USA.
R. Landick, Department of Bacteriology, University of Wisconsin, Madison, WI 53706, USA.

*To whom correspondence should be addressed.

ciencies. We report here observations of the movement of single *E. coli* RNA polymerase molecules along DNA templates. The measurements were made with a microscope-based optical trapping interferometer (9). Calibrated forces were applied in the direction opposing translocation by the polymerase to a small spherical particle (a polystyrene bead) attached to the DNA, while the position of the particle was simultaneously measured. When a sufficiently high force was applied, movement by the enzyme could be stalled, in many cases reversibly. Our results show that this nucleic acid polymerase is a powerful biological motor that can exert considerable force and may operate with energy conversion efficiencies comparable to those of prototypical mechanoenzymes, such as myosin and kinesin.

We conducted experiments using an assay developed (6, 7) to study transcriptional elongation by single molecules of *E. coli* RNA polymerase in vitro (10). Ternary transcription complexes consisting of single molecules of RNA polymerase associated with a DNA template and a nascent RNA transcript were assembled in solution, halted by NTP depletion, and adsorbed onto the cover glass surface of a microscope flow cell. Polystyrene beads (0.52 μm in diameter) were attached to the transcriptionally downstream ends of the DNA molecules so that each bead became tethered to the surface by its connection through the DNA and the polymerase. When supplied with NTPs, up to half of the immobilized transcription complexes are enzymatically active; bead-labeled complexes display elongation kinetics indistinguishable from those of unlabeled complexes in solution (6, 7). In a typical experiment, a transcription complex was first located by video-enhanced, differential interference contrast light microscopy. The complex was identified visually by the Brownian motion of the bead, which was constrained by the length of its DNA tether to a small region centered over the attachment position of the polymerase (6, 7). For the studies described here, the microscope was equipped with an optical trapping interferometer ("optical tweezers" plus a position sensor) that could exert calibrated forces up to ~100 pN on a bead while simultaneously measuring its displacement with subnanometer precision and millisecond time resolution (9, 11). With the laser light shuttered, the optical trap was moved to the region near the bead. The shutter was then opened to activate the trap, and the bead was captured. By adjusting the trap controls, we positioned the center of the bead directly over the polymerase, typically at a height of ~590 nm above the cover glass surface (this particular height was chosen to bring the bead as close as possible to the surface without the risk of touching during subsequent measurements). We then repositioned the trap by moving it at a constant height along the direction of greatest detector sensitivity [the direction defined by the shear axis of the Wollaston prism; see (9, 12)] until the DNA straightened and was held under very light tension, with the bead displaced just 30 to 70 nm from the trap center (Fig. 1A).

We started transcriptional elongation of bead-labeled complexes by exchanging the buffer inside the flow cell with one containing NTPs. In most experiments, elongation was begun immediately before establishment of the initial configuration just described. During elongation, the template was pulled by the stationary polymerase molecule, developing further tension in the DNA between the bead and the polymerase and drawing the bead away from the trap center (Fig. 1B). The optical trap acts as a nearly linear spring of stiffness α_{trap} attached to a stationary reference frame and exerts a force F_{trap} on the bead (Fig. 1C). The bead adopts a position where F_{trap} is balanced by the force F_{tc} exerted by the polymerase, acting through the DNA. The series elasticity due to the DNA, polymerase, and associated linkages acts as a spring of stiffness α_{tc}. By calibrating the optical trap stiffness and determining the displacement of the bead, we could measure F_{trap} and thus F_{tc}. The force could be determined without knowledge of the stiffness α_{tc}, which depends on the length of DNA as well as the applied force (13).

During control experiments in which no NTPs were added, beads remained at an approximately fixed distance from the trap center. Slight changes seen in the interferometer signal (mean rate ~0.3 nm s^{-1} toward the center of the trap) were attributable to instrumental drift.

In elongation experiments using high concentrations of NTPs (1 mM each of adenosine triphosphate, guanosine triphosphate, cytidine 5′-triphosphate, and uridine 5′-triphosphate), 1 μM PP_i, and low trapping force (laser power at specimen, 25 mW; trap stiffness α_{trap}, ~0.03 pN nm^{-1}) (14), we observed continuous movement of beads out to the limit of the usable range of the trap, located roughly 200 nm from the trap center. Once a bead reached this limit, the trap was manually repositioned to bring the bead closer to the trap center so that observation could continue (Fig. 2A). In five of seven elongating complexes studied in this way, beads moved continuously to the limit without stopping, moving at similar velocities after the trap was repositioned. (One complex stopped and failed to restart; another stopped for ~18 s and then continued elongation to the trap limit.) The bead velocity, 4.3 ± 1.3 nm s^{-1} (mean ± SD) (15), was comparable to elongation rates measured under similar conditions in solution (4.4 to 6.8 nm s^{-1}) (6) and in previous microscope experiments (4.2 ± 1.7 nm s^{-1}) (7).

Different behavior was observed when higher trapping forces were used (laser power at specimen, 82 to 107 mW; α_{trap}, ~0.09 to 0.12 pN nm^{-1}). In this regime, 66 of 77 elongating complexes (86%) stopped translocating (stalled) once the bead encountered the high-force region of the trap (Fig. 2, B and C) (16, 17). To test whether stalling was reversible, we maintained the bead at stall, typically for 10 to 15 s, then repositioned the trap center closer to the bead, reducing F_{trap}. After force reduction, 24 of the 66 stalled complexes resumed movement, and some complexes could even be stalled multiple times this way (Fig. 2C). After recovery from stall, the velocity of bead movement in the low-force region of the trap was similar to that

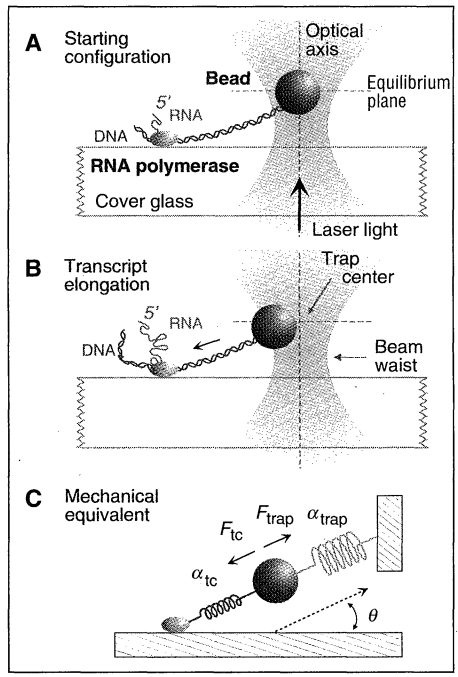

Fig. 1. A cartoon illustrating essential features of the experiment (not to scale). (**A**) The configuration at the start of transcriptional elongation. An RNA polymerase molecule (green ellipsoid) is attached to the cover glass surface of a flow cell. The polymerase is bound to template DNA (red) and has begun to synthesize a transcript RNA (green). A polystyrene bead (blue sphere) is attached to the downstream end of the DNA and is captured and held under slight tension by the light of the optical trap (pink). (**B**) The configuration during subsequent transcriptional elongation. The trap center is located on the optical axis but slightly above the narrow waist of the focused laser beam. The polymerase has proceeded for some distance along the DNA, shortening the segment between the bead and the polymerase. The bead is pulled away from the trap center, increasing the restoring force of the trap. (**C**) The mechanical equivalent of the experimental geometry shown in (A) and (B). All components lie centered in a vertical plane oriented parallel to the Wollaston shear axis.

before stall. The remaining fraction of RNA polymerase molecules stalled irreversibly in that they did not resume elongation when F_{trap} was reduced. Irreversible stalling may be attributable to one or more of several possible causes: The polymerase may have been directly inactivated by the mechanical load, have suffered photodamage from the laser light, or have spontaneously converted into an inactive species ("transcriptional arrest") similar to that formed during transcriptional stalling induced by NTP depletion (*18*, *19*).

The simplest physical interpretation of reversible stalling is that it corresponds to the situation in which F_{trap} has increased to a level where it balances the maximal force that the polymerase can exert (F_{stall}), and no further progress is made. When F_{trap} is reduced, enzyme activity resumes (*20*). During both reversible and irreversible stalls, movement sometimes slowed gradually during the approach to F_{stall} (for example, the third stall in Fig. 2C), whereas in other cases movement continued at nearly constant velocity, slowing abruptly close to F_{stall} (for example, the first and second stalls in Fig. 2C). Transcription complexes display differing biochemical properties depending on the nucleotide sequence of the DNA to which they are bound (*21*). Abrupt reversible stalling may correspond to the arrival of the enzyme at a template position for which F_{stall} is somewhat lower than that of the preceding positions, producing rapid arrest. This interpretation also could explain why F_{stall} values determined for multiple stalls of a single complex often differed by more than the experimental uncertainty in measurement (*22*). It is tempting to speculate that some sites of abrupt stalling might correspond to DNA sequences that trigger cycles of discontinuous elongation (*2*, *3*) or "jumping." At such sequences, a portion of the RNA polymerase molecule may, during a single nucleotide addition cycle, move along the DNA by ~10 bp, an axial distance of ~3.4 nm (*23*). These large movements of the enzyme would be expected, all else being equal, to give stall forces significantly lower than those of single base pair movements, because the free energy available from nucleotide addition would be applied over a larger distance. Nucleotide sequence effects on behavior under mechanical load could be studied in future experiments through the use of DNA templates containing homopolymer tracts or direct repeats.

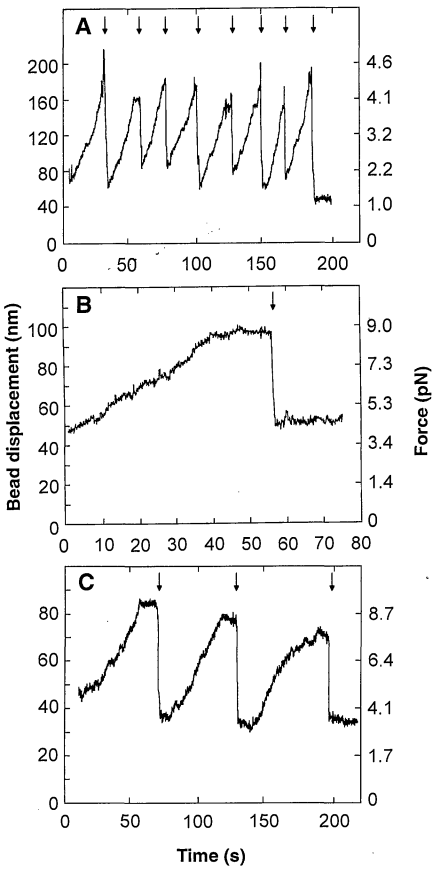

Fig. 2. Time courses for displacement from the trap center and the corresponding optical force applied to single beads driven by translocation of an RNA polymerase molecule along DNA. Force scales (right-hand axes) are nonlinear (*14*). The zero of the time axis is arbitrary. Reactions were conducted at 1 mM NTPs with 0.001 mM (**A**) or 1 mM (**B** and **C**) PP_i at laser powers of 25 (A), 82 (B), or 99 (C) mW. Vertical arrows designate times at which the trap was repositioned to reduce the optical force. An irreversible stall is shown in (B), and reversible stalls (first two stalls) and an irreversible stall (third stall) are shown in (C).

The distributions of F_{stall} values were obtained at 1 mM NTPs with 1 μM PP_i. The distributions of reversible and irreversible stall forces were statistically indistinguishable, with values of 13.0 ± 4.0 pN (mean ± SD, n = 8) and 12.6 ± 3.5 pN (n = 14), respectively. A possible explanation for the similarity of the distributions is that the reversibly stalled state is a precursor of the irreversibly stalled state. In this view, most or all of the stalled complexes are initially stalled reversibly, but a fraction of these are subsequently inactivated and therefore fail to resume elongation when F_{trap} is reduced.

F_{stall} was also determined at two higher concentrations of PP_i (0.5 and 1 mM) with 1 mM NTPs. Increasing the PP_i concentration to 1 mM slowed transcriptional elongation by about twofold (*24*), but F_{stall} remained nearly constant [at 0.5 mM PP_i, 13.0 ± 4.1 pN (n = 5) for reversible and 13.1 ± 2.6 pN (n = 10) for irreversible stalls; at 1.0 mM PP_i, 11.5 ± 2.9 pN (n = 11) for reversible and 9.9 ± 3.4 pN (n = 18) for irreversible stalls]; this observation may place important constraints on the RNA polymerase force-generation mechanism. In light of this result, stalls observed at all PP_i concentrations were pooled (Fig. 3A) to generate a global distribution with mean F_{stall} = 12.3 ± 3.5 pN (n = 24) for all reversible stalls. We previously found that single immobilized transcription complexes exhibit a range of velocities (*7*). Such heterogeneity among complexes may also contribute to the width of F_{stall} distributions. The polymerase is fixed to the glass at random and presumably is not free to rotate. Different spatial orientations of the polymerase with respect to the direction of the applied force might also cause F_{stall} to vary from molecule to molecule. A small fraction of the complexes did not stall before reaching the limit of the usable range of the trap (Fig. 3B). The assumption that these complexes would stall at a force larger than the maximum measurable force at the laser power used yields a lower limit estimate of 13.6 pN for the mean reversible F_{stall} (*25*). Despite systematic instrumentation errors for these measurements estimated at ~30% (*22*), the F_{stall} values for single RNA polymerase molecules are clearly much larger than are forces previously measured for single molecules of other mechanoenzymes: up to 6 pN for kinesin (*26*) and 3 to 5 pN for myosin (*27*).

The efficiency of chemomechanical energy conversion in RNA polymerase may be defined as the fraction of the total free energy change of the chemical RNA polymerization reaction ($\Delta G'_{polym}$) that the enzyme expends to perform mechanical work against an external load. Thermodynamically reversible motors are most efficient as they approach the point of stalling. The free energy available from the chemical reaction varies with the PP_i-to-NTP concentration ratio because these are the product and

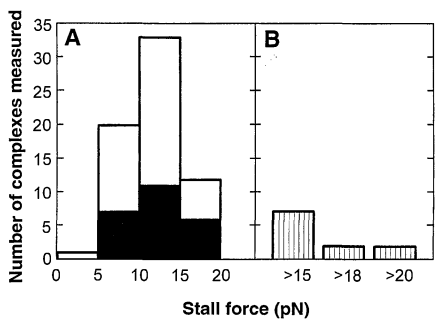

Fig. 3. Stall force distributions measured from pooled data obtained at 1 mM NTPs with 0.001, 0.5, and 1.0 mM PP_i. For beads exhibiting reversible stalls, only data from the first stall were included. Laser powers (and corresponding maximum measurable forces) of 82 mW (15 pN), 99 mW (18 pN), and 107 mW (20 pN) were used in 25, 33, and 19 measurements, respectively. (**A**) Stacked histogram of stall forces for irreversible (open portion of bars, n = 42) and reversible (solid portion of bars, n = 24) stalls. (**B**) Histogram of estimated lower bound of stall forces for complexes (n = 11) that did not stall before exiting the calibrated range of the trap. The number below each bar represents the maximum measurable force for the laser power used.

reactant species, respectively. For the conditions used, $\Delta G'_{polym}$ ranged from −7.2 kcal mol^{-1} (at 1 μM PP_i) to −3.1 kcal mol^{-1} (at 1 μM PP_i) (*1*). Under the assumption that each NTP consumed advances the polymerase 1 bp on average along the DNA (0.34 nm along the DNA axis), the mean F_{stall} estimate corresponds to maximal energy conversion efficiencies of 9, 19, and 22% at 0.001, 0.5, and 1 mM PP_i, respectively. These efficiencies are comparable to values obtained for biological motors such as kinesin [40 to 60% (*11*, *28*)] or myosin [12 to 42% (*27*)] (*29*).

Nucleic acid polymerases carry out biosynthetic reactions and are not ordinarily classified as mechanoenzymes. Nevertheless, our results indicate that individual molecules of *E. coli* RNA polymerase exert forces and operate with energy conversion efficiencies that are similar to those of prototypical mechanoenzymes, whose specialized function is to generate biologically useful force and motion. Inside living cells, interactions between transcription complexes and cellular structures or DNA-bound proteins create substantial forces that oppose the translocation of polymerases relative to DNA (*4*, *5*). For example, to function in opposition to loads imposed by transcription-induced supercoiling of plasmid DNA in vivo, *E. coli* RNA polymerase must generate forces estimated at ~6 pN (*30*). Forces of this magnitude are sufficient, for example, to stall solitary molecules of kinesin or myosin, but are nonetheless smaller than the forces achieved by RNA polymerase molecules in vitro. We anticipate that further development of optical measurements on single transcription complexes will allow detailed characterization of the multiple mechanical processes (*2*, *3*, *23*) by which RNA polymerase moves along DNA.

REFERENCES AND NOTES

1. T. D. Yager and P. H. von Hippel, in Escherichia coli *and* Salmonella typhimurium: *Cellular and Molecular Biology*, F. C. Neidhardt *et al.*, Eds. (American Society for Microbiology, Washington DC, 1987), vol. **2**, pp. 1241–1275; D. A. Erie, T. D. Yager, P. H. von Hippel, *Annu. Rev. Biophys. Biomol. Struct.* **21**, 379 (1992).
2. C. L. Chan and R. Landick, in *Transcription: Mechanism and Regulation*, R. Conaway and J. Conaway, Eds. (Raven, New York, 1994), pp. 297–320.
3. M. J. Chamberlin, in *The Harvey Lectures* (Wiley-Liss, New York, 1994), Ser. **88**, pp. 1–21.
4. P. R. Cook, *Bioessays* **16**, 425 (1994).
5. J. C. Wang, in *Transcriptional Regulation*, S. L. McKnight and K. R. Yamamoto, Eds. (Cold Spring Harbor Laboratory Press, Cold Spring Harbor, NY, 1992), pp. 1253–1269; D. N. Cook, D. Ma, J. E. Hearst, in *Nucleic Acids and Molecular Biology*, F. Eckstein and D. M. J. Lilley, Eds. (Springer-Verlag, Berlin, 1994), vol. 8, pp. 133–146.
6. D. A. Schafer, J. Gelles, M. P. Sheetz, R. Landick, *Nature* **352**, 444 (1991).
7. H. Yin, R. Landick, J. Gelles, *Biophys. J.* **67**, 2468 (1994).
8. H. Kabata *et al.*, *Science* **262**, 1561 (1993).
9. K. Svoboda, C. F. Schmidt, B. J. Schnapp, S. M. Block, *Nature* **365**, 721 (1993).
10. Sample preparation methods, buffers, and reaction conditions were the same as those used previously (*7*), except that disodium pyrophosphate (Sigma) was added at the specified concentration together with the NTPs, and 0.52-μm-diameter carboxylated polystyrene beads (Polysciences, Warrington, PA) were used in place of 0.226-μm beads. DNA template no. 5 (*6*), which contains the strong T7 A1 promoter followed by 3908 downstream base pairs, was used in all experiments. Transcription complex surface density was measured and controlled as in (*7*), so that each bead had a probability ≤0.20 of being attached to more than one transcription complex.
11. K. Svoboda and S. M. Block, *Cell* **77**, 773 (1994).
12. ———, *Annu. Rev. Biophys. Biomol. Struct.* **23**, 247 (1994).
13. S. B. Smith, L. Finzi, C. Bustamante, *Science* **258**, 1122 (1992); C. Bustamante, J. F. Marko, E. D. Siggia, S. Smith, *ibid.* **265**, 1599 (1994). More complete characterization of the series elastic spring constant α_{tc} (which includes contributions from the stiffness of the DNA as well as from the stiffness of other structures, such as the polymerase, through which the DNA is linked to the cover slip) could be used to simultaneously measure both the force and velocity generated by the polymerase, as has been done for kinesin (*11*). A complication of this approach is the fact that α_{tc} has a time-varying component, due to the changing length of the DNA tether.
14. We calibrated trap stiffness (α_{trap}) using free beads, either by measuring the power spectrum of the Brownian motion or by measuring the bead displacement from the trap center produced by viscous drag forces (*9*, *11*, *12*). Stiffnesses obtained with the use of these two methods differed by <10% for excursions below half the usable detector range (<100 nm). For larger excursions, the drag force method was used exclusively. Calibration was accomplished in two stages. First, the relation between digitized interferometer output voltage and true displacement (in nanometers) was established as described previously (*9*). Second, the relation between trapping force (in piconewtons) and displacement (in nanometers) was determined by the drag force method, with viscous forces being corrected for the proximity of the cover glass surface (*12*). The two data sets were then combined. In contrast to the case of silica particles (*11*), the force-displacement relation for polystyrene beads has significant nonlinearities in the outermost part of the trap; therefore, calibration data out to 150 nm were fit by a fifth-order polynomial to extrapolate interferometer signals into the region between 150 nm and ~200 nm. This procedure may miscalculate the actual force produced in the region beyond 150 nm; however, exclusion from the analysis of data taken in this region did not significantly alter the mean stall forces reported here. The estimated force at 200 nm displacement was taken to be the largest measurable force at a given laser power.
15. A correction for the contribution of tether elasticity (spring constant α_{tc}) has not been applied to the bead velocity measurement. Therefore, this bead velocity represents a lower bound on the polymerase elongation rate.
16. Interferometer output was low-pass–filtered at 1 kHz and digitized at 1-ms intervals. Before analysis, records were averaged in blocks of 100 points to give a final time resolution of 100 ms. Bead velocity (v_{bead}) was measured as the slope of the line fit to bead position versus time within a 10-s sliding window. Beads achieving $v_{bead} \geq 0.6$ nm s^{-1} continuously for ≥5 s (positive velocity being defined as movement away from the trap center) were judged to be attached to functional transcription complexes and were selected for further analysis. Any interval during which v_{bead} was <0.6 nm s^{-1} continuously for ≥5 s was taken to represent a stall. By this criterion, 13 of 77 complexes spontaneously underwent brief transient stalls that were apparently uncorrelated with the amount of force and were excluded from subsequent analyses. Such events may correspond to transcriptional pausing (*1*, *2*) because movement resumed without the trap being repositioned.
17. Initially, 87 elongating complexes were observed at high laser powers. However, in 10 of them the bead spontaneously detached from its tether before the trap could be repositioned. The site of breakage could not be determined. Data from such complexes were excluded from further analysis. Eleven of the remaining 77 complexes did not stall before reaching the limit of the usable range of the trap.
18. D. A. Erie, O. Hajiseyedjavadi, M. C. Young, P. H. von Hippel, *Science* **262**, 867 (1993).
19. Although inactive enzyme species induced by chemical stalling in solution can be reactivated by GreB protein [S. Borukhov, V. Sagitov, A. Goldfarb, *Cell* **72**, 459 (1993)], the fraction of complexes that were irreversibly stalled by mechanical load did not decrease when 100 nM GreB protein was included in the buffer (*24*), which suggests either that these complexes are in a different state than that produced in the chemical stalling experiments or that GreB cannot act on complexes adsorbed to cover slips.
20. It is unlikely that the reversible stalling events are due to radiation-induced damage to RNA polymerase, because enzyme photodamage is generally irreversible. The view that reversible stalls are due to applied force, not laser irradiation alone, is further supported by the observation that 95% of reversibly stalled complexes resumed bead movement shortly after the trap was repositioned. Repositioning the trap decreases F_{trap} but increases the laser intensity at the RNA polymerase because the trap is moved closer to the enzyme molecule. Control experiments [at laser powers 82 to 99 mW; all reported laser powers are estimates in the specimen plane determined by the method of (*11*)] in which the trap was repositioned before the stall (in 14 of 15 complexes) subjected the transcription complexes to higher average light intensities and lower average trap forces than those in the stalling experiments. In the controls, complexes were inactivated in 82 ± 58 s (mean ± SD, $n = 15$) exposure to the laser, whereas in the stalling experiments first stalls (reversible or irreversible) occurred significantly earlier, in 38 ± 16 s (mean ± SD, $n = 66$), confirming that the first stalls cannot be explained by photodamage alone.
21. B. Krummel and M. J. Chamberlin, *J. Mol. Biol.* **225**, 221 (1992).
22. Stall force measurements are subject to systematic errors, which we attempted to estimate. The two primary sources of error have opposing effects and arise from the fact that the bead motion is not strictly parallel to the cover glass surface but has a vertical component. During elongation, beads experience a force directed downward at an angle θ, where θ is the angle between the DNA and the cover glass (Fig. 1C). This angle varies continuously during the course of an experiment as the DNA tether shortens. Neglect of the downward force component will cause underestimation of the actual force produced by the polymerase by a factor (cosθ). The minimal DNA tether length at stall was estimated by video analysis of the bead Brownian motion (*7*) with the trap shuttered. The tether length was >1915 bp (651 nm) in all experiments, corresponding to $\theta < 41°$. This geometrical consideration alone would lead to a value for F_{stall} that underestimates the applied force by a variable amount up to ~24%. A second source of systematic error, which has the opposite sign, arises from the fact that the interferometer is most sensitive to motion in the plane of the laser beam waist and along the Wollaston shear direction. Polystyrene spheres are initially trapped at a point slightly above the position of the true beam waist (Fig. 1B), and the downward force component acting along the DNA has the effect of carrying the bead into the region of greater detector sensitivity (in contrast, viscous drag calibration experiments, in which purely horizontal forces are generated, are not subject to this artifact). This leads to an overestimate of the distance moved, hence to an overestimate of the force F_{stall}. We estimated the magnitude of this effect at 26% or less, based on experiments in which beads fixed to a cover glass were moved in the specimen plane through the detector at various heights relative to the laser beam waist (*24*). Yet other uncertainties arise because the trap stiffness, hence the restoring force, varies with height, the trap being weaker in the vertical direction than in the horizontal direction. Given these various

opposing effects, it seems reasonable to estimate the overall systematic errors in force at ≤~30%.

23. B. Krummel and M. J. Chamberlin, *J. Mol. Biol.* **225**, 239 (1995); E. Nudler, A. Goldfarb, M. Kashlev, *Science* **265**, 793 (1994); D. Wang *et al.*, *Cell* **81**, 341 (1995); E. Nudler, M. Kashlev, V. Nikiforov, A. Goldfarb, *ibid.*, p. 351.
24. H. Yin *et al.*, data not shown.
25. This estimate is a lower limit because it includes data from complexes that did not stall before reaching the trap limit and because we cannot exclude the possibility that some events classified as stalls may in fact be lengthy transcriptional pauses (*16*).
26. S. M. Block, *Trends Cell Biol.* **5**, 169 (1995).
27. J. T. Finer, R. M. Simmons, J. A. Spudich, *Nature* **368**, 113 (1994); J. T. Finer, A. D. Mehta, J. A. Spudich, *Biophys. J.* **68**, 291s (1995); A. Ishijima *et al.*, *Biochem. Biophys. Res. Commun.* **199**, 1057 (1994); H. Miyata *et al.*, *Biophys. J.* **68**, 286s (1995).
28. A. J. Hunt, F. Gittes, J. Howard, *Biophys. J.* **67**, 766 (1994).
29. Underestimation of F_{stall} (*25*) will cause underestimation of the maximum energy conversion efficiency. Moreover, our efficiency calculation assumes that stalling occurs when the free energy available to drive movement in one cycle of the chemical reaction balances the free energy required to translocate 1 bp along the DNA against the applied force. However, stalling could also occur because of structural alterations in the transcription complex (for example, stabilization of a catalytically inactive enzyme conformation by the applied force). In that case, the maximum efficiency calculated from F_{stall} would underestimate the true efficiency. In contrast, enzymatic consumption of NTPs uncoupled to translocation would reduce the energy conversion efficiency below that calculated from F_{stall}. Although little such consumption has been reported for transcription complexes in solution [for example, see M. Chamberlin, R. L. Baldwin, P. Berg, *J. Mol. Biol.* **7**, 334 (1963)], we cannot exclude the possibility that such uncoupled reactions are catalyzed by immobilized enzyme molecules subjected to the high applied forces used in the stalling experiments. Estimates of energy conversion efficiency from the stall forces of single kinesin and myosin molecules carry analogous uncertainties. Recent evidence (*11*) suggests that kinesin is not tightly coupled near stall.
30. *Escherichia coli* plasmids that carry multiple transcription units can accumulate high densities of transcription-induced supercoils (*31*). This effect can be observed in the absence of DNA gyrase or topoisomerase I activities (which relax negative or positive supercoils, respectively) when one or more of the transcribed genes encodes a membrane-interacting protein (*5*). Specific linking differences (σ) of −0.013 in topoisomerase I mutants [D. N. Cook, D. Ma, N. G. Pon, J. E. Hearst, *Proc. Natl. Acad. Sci. U.S.A.* **89**, 10603 (1992)] and 0.024 in the presence of a DNA gyrase inhibitor [H. Y. Wu, S. H. Shyy, J. C. Wang, L. F. Liu, *Cell* **53**, 433 (1988)] have been reported. RNA polymerase transcription is accompanied by an obligatory rotation relative to the DNA helix. Therefore, the supercoiling torque τ_s [($|\sigma|$) 1.4×10^{-19} N m rad^{-1} (*31*)] is expected to exert a force opposing translocation that is estimated by $F_s = 2\pi\tau_s/h$, where h is the pitch of the DNA helix, 3.6 nm. F_s = 3 and 6 pN, respectively, in the two cited cases. However, this calculation may underestimate the force by a factor of ~2 because supercoils in vivo are thought to be confined to a limited portion of the plasmid DNA.
31. L. F. Liu and J. C. Wang, *Proc. Natl. Acad. Sci. U.S.A.* **84**, 7024 (1987).
32. Supported by grants from the National Institute of General Medical Sciences to J.G., R.L., and S.M.B. M.D.W. was supported by a Damon Runyon–Walter Winchell Cancer Research Fund postdoctoral fellowship. K.S. and S.M.B. thank the Rowland Institute for Science for support during the early stages of this work. A movie of the experiment shown in Fig. 2A can be viewed on the World Wide Web at http://www.rose.brandeis.edu/users/gelles/stall/.

11 August 1995; accepted 26 October 1995

Minimization of a Polypeptide Hormone

Bing Li, Jeff Y. K. Tom, David Oare, Randy Yen, Wayne J. Fairbrother, James A. Wells,* Brian C. Cunningham*

A stepwise approach for reducing the size of a polypeptide hormone, atrial natriuretic peptide (ANP), from 28 residues to 15 while retaining high biopotency is described. Systematic structural and functional analysis identified a discontinuous functional epitope for receptor binding and activation, most of which was placed onto a smaller ring (Cys^6 to Cys^{17}) that was created by repositioning the ANP native disulfide bond (Cys^7 to Cys^{23}). High affinity was subsequently restored by optimizing the remaining noncritical residues by means of phage display. Residues that flanked the mini-ring structure were then deleted in stages, and affinity losses were rectified by additional phage-sorting experiments. Thus, structural and functional data on hormones, coupled with phage display methods, can be used to shrink the hormones to moieties more amenable to small-molecule design.

The generation of leads for drug design is usually achieved through a laborious discovery process wherein a large number of small molecules are screened for binding to a particular receptor or for modulation of a particular biological response. Although structure-based approaches have been used in some cases for generating candidate molecules directly (*1*), this approach has been limited to binding sites for small substrate molecules or short, continuous peptide segments.

Protein-protein interactions are crucial events in most biological processes and are therefore important targets for drug design. Such interfaces are generally large (600 to more than 1300 Å^2), with 10 to 30 contact side chains on each side of the interface (*2*). Moreover, each patch of contact residues is presented from peptide segments that are often distant in primary sequence. Mimicking such large and discontinuous binding surfaces with rationally designed small molecules is a daunting prospect, but it may be simplified because only a small subset of contact side chains appears to be necessary for tight binding at these interfaces (*3*). Displaying these functional epitopes on minimal structured scaffolds may permit smaller candidate compounds to be generated that bind at protein-protein interfaces.

Atrial natriuretic peptide is a 28-residue peptide hormone that is important for regulation of blood pressure and salt balance (*4*). Smaller ANP peptides produced by the screening of synthetic analogs are at least 500 times weaker in receptor-binding affinity (*5*). It is likely that the binding of ANP to its signaling receptor is highly sensitive to the conformation of ANP, as indicated by the loss of binding caused by the reduction of its single disulfide bond. Using a constrained scaffold designed to preserve the structural presentation of the critical binding determinants, we present a systematic strategy for reducing the size of ANP while maintaining high binding affinity and biopotency.

The first step in our minimization process (Fig. 1) was to determine which ANP residues are important for binding to the extracellular domain of the natriuretic peptide receptor–A (NPR-A) by alanine-scanning mutagenesis (*6*). Each of the 28 residues in ANP was converted to alanine, except those comprising the Cys^7 to Cys^{23} disulfide and Ala^{17}. An enzyme-linked immunosorbent assay (ELISA) of these ANP mutants, produced as peptide fusions with gene III coat protein on phage (*7*), allowed us to rapidly assess the relative binding affinity of the mutants by eliminating the need to purify each peptide to homogeneity. Mutations at only seven positions (Phe^8, Met^{12}, Asp^{13}, Arg^{14}, Ile^{15}, Leu^{21}, and Arg^{27}) each resulted in an affinity that was more than 10 times lower than that of wild-type ANP (Fig. 2). These results are consistent with effects on an aortic ring contraction assay reported for substitutions with D-amino acids or alanines in ANP (*8*).

Five of the seven most important residues (Phe^8, Met^{12}, Asp^{13}, Arg^{14}, and Ile^{15}) formed a small functional epitope on one side of the hormone (Fig. 3A). On the basis of the structure of ANP (*9*), three alternative disulfide forms of the molecule (Cys^7 to Cys^{17}, Cys^6 to Cys^{17}, and Cys^5 to Cys^{17}) were designed to isolate this functional epitope on a smaller disulfide ring and eliminate the native Cys^7 to Cys^{23} disulfide (Fig. 3B). Of these three variants, Cys^6 to Cys^{17} was the best, albeit with an affinity that was more than 100 times lower than

B. Li, W. J. Fairbrother, J. A. Wells, B. C. Cunningham, Department of Protein Engineering, Genentech, 460 Point San Bruno Boulevard, South San Francisco, CA 94080, USA.
J. Y. K. Tom and D. Oare, Bioorganic Chemistry, Genentech, 460 Point San Bruno Boulevard, South San Francisco, CA 94080, USA.
R. Yen, Medicinal and Analytical Chemistry, Genentech, 460 Point San Bruno Boulevard, South San Francisco, CA 94080, USA.

*To whom correspondence should be addressed.